Am J Cancer Res 2019;9(10):2209-2215
www.ajcr.us /ISSN:2156-6976/ajcr0102338

Original Article

Modeling multi-needle injection into solid tumor

Vladimir Subbotin[1], Gennady Fiksel[2]

[1]602 Samuel Drive, Madison, WI 53717, USA; [2]1035 Heather Way, Ann Arbor, MI 48104, USA

Received September 15, 2019; Accepted September 30, 2019; Epub October 1, 2019; Published October 15, 2019

Abstract: The discovery of mechanisms by which the cancer cells avoid the host immune attack (immune checkpoints) as well the capability of the monoclonal antibodies (mAbs) to blockade the checkpoint proteins on cancer and tumor-infiltrating cells (CTLA-4, PD-1, and PD-L1) promised new breakthroughs in the cure of cancer. After these mechanisms of cancer escaping the host immunity were undoubtedly confirmed in numerous experimental and clinical studies, the FDA approval of CTLA-4 and PD-1/PD-L1 mAbs for systemic treatment thought to revolutionize the outcome of cancer treatment. However, as of today, the anticipated curative effect of anti-CTLA-4 and PD-1/PD-L1 mAb treatments has been observed only in a small population of patients. In addition, systemic administration of mAbs in clinics has been found associated with new toxicity profiles, sometimes very severe. The main obstacle that hinders the mAbs therapy appears to be the inability of delivering mAbs to a sufficient number of cancer cells and tumor infiltrating cells. As an alternative to the systemic administration (or as a complement to it), local intratumoral delivery of mAbs has been anticipated to resolve that issue. However, unlike the systemic mAbs administration, for which formidable but surmountable obstacles (big size of mAbs ~150 kD, high interstitial fluid pressure in solid tumors, etc.) have been known to hamper mAbs delivery to cancer and tumor-infiltrating cells, the lack of effects of intratumoral mAbs administration remains completely incomprehensible and needs a new theoretical reconsideration that we have attempted in our analysis. It can be suggested that the limited benefits of the intratumoral mAbs administration appeared to be rooted in the same problem that hindered the effects of systemic mAbs administration: the inability to reach a sufficient number of cancer cells and tumor-infiltrating cells. We hypothesize that the core of the problem stems from the fact that the single-needle intratumoral injection forms a very localized, jet-like distribution of the drug (mAbs) that constitutes only a small fraction of the total volume of the tumor. In this light we are re-evaluating the theoretical reasonableness of the single-needle intratumoral injection approach. We propose that multi-needle injection will circumvent this limitation and for that we analyze the behavior of an injectant in tissues using different configurations of the injection needles. To accomplish this goal, we created a model of injectant distribution in a solid tissue based on the traditional technique of single-needle injection and then extended that model to a case of simultaneous multi-needle injection. To develop the model of drug delivery and transport in biological tissues, we followed a frequently used approach of modeling the diffusive transport of liquid through a porous media using the Darcy's law that relates the flow velocity, the pressure gradient, and the tissue permeability. The analysis demonstrates that a multi-needle injection setup provides a significantly more widespread and homogeneous injectant distribution within a solid tumor than that for a single needle injection for the same tumor size. Adding separate draining needles can further improve the delivery of injectant to cancer and tumor-infiltrating cells.

Keywords: Cancer, immunotherapy, checkpoint inhibition, mAbs, intratumoral injection, liquid transport, solid tumor

Introduction

Recent groundbreaking discovery of mechanisms, by which cancer cells avoid the host immune attack (immune checkpoints), has revolutionized cancer treatment. Both experimental and clinical results have clearly demonstrated that the blockade of checkpoint proteins with CTLA-4 and PD-1/PD-L1 monoclonal antibodies (mAbs) is capable of activating the immune system and generate anti-tumor response. Recently, systemic intravenous infusion therapies with CTLA-4 and PD-1/PD-L1 antibodies [1, 2], have received the FDA approval (for review see) [3, 4]. However, the benefits of anti-CTLA-4 and PD-1/PD-L1 treatments have been observed only in a small population of patients [5, 6], while systemic administration of mAbs in clinic research has been found to be associated with new toxicity profiles [7-9], sometimes very severe [10].

The main explanation for the limited effects of systemic mAbs administration was a failure to

deliver the mAbs to sufficient number of cancer and tumor-infiltrating cells. The local intratumoral injection of mAbs using a routine syringe/single needle technique was developed that significantly decreased risk of toxic side effects [11], and results from the Sondel Laboratory (University of Wisconsin) [12] and other groups, e.g. [13], clearly demonstrated the superiority of local intratumoral administration compared to the systemic administration. Along with the confirmed knowledge of how cancer cells escape the anti-tumor immune response, i.e. characterization of checkpoint proteins and availability of corresponding mAbs, a local intratumoral delivery of mAbs has been anticipated to bring a treatment solution on a much greater scale than had been achieved previously [11, 14-16].

However, unlike the systemic mAbs administration, for which formidable but surmountable obstacles (big size of mAbs ~150 kD, high interstitial fluid pressure in solid tumors, etc.) have been known to hamper mAbs delivery to cancer and tumor-infiltrating cells, the lack of effects of intratumoral mAbs administration remains completely incomprehensible and needs a new theoretical reconsideration that we have attempted in our analysis.

It can be suggested that the limited benefits of the intratumoral mAbs administration appeared to be rooted in the same problem that hindered the effects of systemic mAbs administration: the inability to reach a sufficient number of cancer and tumor-infiltration cells. Even when consecutive injections into different tumor regions were done without a complete retraction of the needle tip from the tumor, as in recent experiments [17], it also has not brought significant benefits.

We hypothesize that the core of the problem stems from the fact that the single-needle intratumoral injection forms a very localized, jet-like distribution of the drug (mAbs) that constitutes only a small fraction of the total volume of the tumor. In this light we are re-evaluating the theoretical reasonableness of the single-needle intratumoral injection approach. We propose that multi-needle injection can circumvent this limitation, and analyze the behavior of injectant using different configurations of the injection needles.

To accomplish this goal, we created a model of injectant distribution in a solid tissue based on the traditional technique of single-needle injection and then extended that model to a case of simultaneous multi-needle injection. To develop the model of drug delivery and transport in biological tissues, we followed a frequently used approach of modeling the diffusive transport of liquid through a porous media using the Darcy's law that relates the flow velocity, the pressure gradient, and the tissue permeability. The main difference between the two methods of medication delivery - via needle injection and via slow diffusive inward transport from the multiple points of tissue interstitium is that the former occurs at a much higher flow velocity and pressure. It turns outs, that at a high enough pressure and/or velocity, the permeability of the tissues is modified by the flow itself. It was noted and experimentally investigated in [18] for example, where this effect was coined as "cracking", due to a similarity to the geological structures cracking under the influence of high-pressure water jets. The difference between the permeability values published in literature and measured in [18] is very large, reaching a factor between 100 and 1000 due to the "creation of a connecting network of microcracks" [18].

In our paper, we apply the ideas developed by the authors of [18] and solve the transport model with the permeability adjusted to match their experimental results. In addition, we further extend their model by assuming that the permeability modification is anisotropic, that is much higher it the direction of the flow than in the perpendicular direction. This is done to match the experimental observations, also published in [18] as well as in many other articles, of jet-like propagation of the injected liquid.

The model was solved using the ®COMSOL Multiphysics package. We explored three delivery scenarios: a) single needle injection, b) multi (7)- needle injection, and c) multi-needle injection with an addition of several (6) drainage needles. It is shown that increasing the number of the needles results in a much better uniformity of the drug distribution throughout the volume of the modeled tumor. Introduction of the drainage needles further improves the uniformity of the drug distribution and makes it undependable on the opacity and the porosity

of the tumor's shell (capsule). Although a particular number of needles - 7 for the injection and 6 for the drainage - is used in this paper, our simulations indicated that a specific choice for the quantity of these needles is not important as a long as they cover a large fraction of the tumor cross-section.

Transport model

The drug delivery and transport in biological tissues is frequently described using a transport model of liquid through a porous media. Typically it is modeled using the Darcy's law that relates the flow velocity u with the pressure gradient ∇p

$$u = -\frac{k}{\mu}\nabla p = -K\nabla p \quad (1)$$

where k [m^2] is the media permeability, μ [Pa s] is the liquid dynamic viscosity, and K [m^2 Pa^{-1} s^{-1}] = k/μ is the hydraulic conductivity [19].

The measured values of the hydraulic conductivity vary widely and they strongly depend on the nature and the composition of the tissue. For example, the reported values for the adipose tissues vary between 10^{-12} m^2 Pa^{-1} s^{-1} and 10^{-13} m^2 Pa^{-1} s^{-1} [20]. The uncertainty is even higher for very non-uniform and case-to-case different tumor tissues. Therefore, at best, the results of such modeling could be taken only as an order-of-magnitude approximation.

Nevertheless, these types of modeling can be and have been applied for the slow inward drug infusion during intravenous therapies. However, a straight- forward application of that model fails when applied to delivery methods using needle injection directly into the tumor. That can be illustrated by estimating the pressure near the needle tip that is needed to sustain a certain injection flow rate. It can be done by using Eq. 1 and substituting $u \approx Q/\pi a_n^2$ and $\nabla p \approx p/a_n$,

$$p = \frac{Q}{\pi a_n K} \quad (2)$$

where a_n is the radius of the needle opening and Q is the injection flow rate. Assuming an injection flow rate of Q = 10 mm^3/s and a needle with a_n = 0.1 mm (gauge 27) results in a hydrostatic pressure of 3 × 10^4 kPa-3 × 10^5 kPa or between 300 atm and 3,000 atm, which of course is unrealistic.

This estimate also contradicts direct measurements of the injection pressure described in [18]. The measurements indicate that a pressure necessary to sustain a flow rate of 10 mm^3/s is about 30-40 kPa a factor of ~1,000-10,000 lower than the above estimate, and that the dependance of the pressure on the injection rate is almost linear - $p = CQ$ with a slope of C = 740 $GPasm^{-3}$.

From these published results it is possible to estimate the tissue conductivity using a simple model of the liquid expansion. Assume that near the needle tip the flow is uniform so the flow velocity can be expressed as $u = Q/\pi a_n^2$ that away from the tip the flow expands spherically so the flow velocity can be expressed as $u = Q/4\pi r^2$. Both expressions can be combined to describe the flow velocity by a single continuous function $u = Q/\pi (a_n^2+4r^2)$ and rewrite Eq. 1 as

$$\frac{Q}{\pi a_n^2 + 4\pi r^2} = -K\nabla p \quad (3)$$

This equation can be integrated from 0 to ∞ to obtain an estimate for the hydraulic conductivity of

$$K = \frac{1}{4Ca_n} = 3.4 \times 10^{-9}\ m^2\ Pa^{-1}\ s^{-1} \quad (4)$$

which is several orders of magnitude higher than the published values [20].

It was suggested in [18] that this discrepancy can be a result of a modification of the tissue by the liquid flow itself, similar to the effect of "cracking" that is observed during a high-pressure liquid transport trough a geological formation. To further develop this model, we also assume that the "cracking" is anisotropic, in other words that is it happens primarily in the direction of the flow. Specifically, assume for simplicity that the conductivity in the direction of the flow is $K_{\parallel}$ = 3.4 × 10^{-9} m^2 Pa^{-1} s^{-1} while in the perpendicular direction it is at an unmodified value of $K_{\perp}$ = 10^{-12} m^2 Pa^{-1} s^{-1}.

Numerical simulations

In this section we described the results of multi-needle injection using the transport model described in the previous section. The simulations were done using the ®COMSOL Multiphysics package.

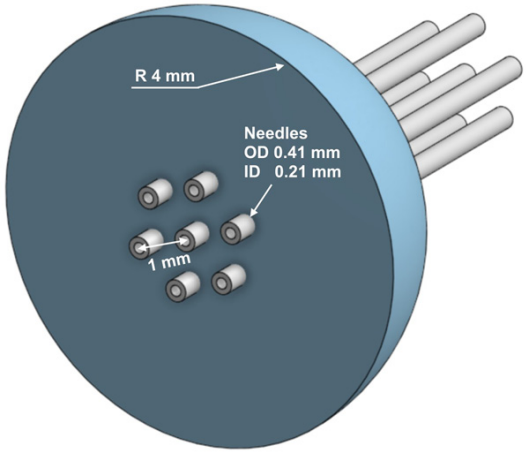

Figure 1. Multiple needle setup. The tumor tissue is modeled by a porous media enclosed in a sphere with a radius of 4 mm. The front part of the sphere is not shown for clarity. Seven 27-gauge needles with an OD of 0.41 mm and an ID of 0.21 mm are inserted with their tips positioned at the equatorial cross-section. The six needles surrounding the central needle are positioned on a circle with a radius of 1 mm.

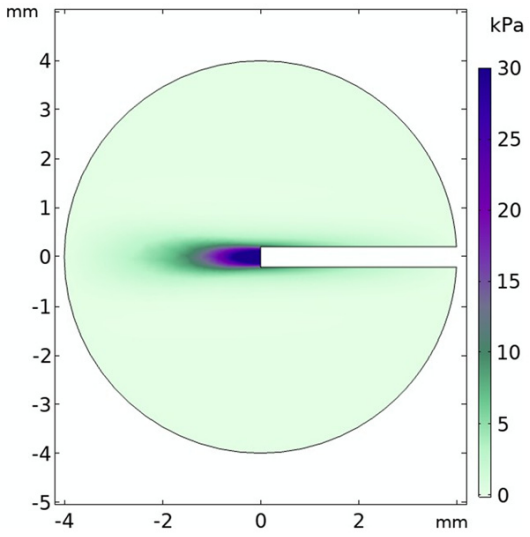

Figure 2. Single needle setup. Pressure map across the equatorial cross-section.

The multi-needle setup is shown in **Figure 1**. The injected tissue is modeled by a sphere with a radius of 4 mm. The tissue media is porous, with the hydraulic conductivity specified according to the previous section. Seven 27-gauge needles with an OD of 0.41 mm and an ID of 0.21 mm were inserted into the tumor with their tips positioned at the center. The six needles surrounding the central needle are positioned on a circle with a radius of 1 mm. The front part of the sphere is not shown for clarity.

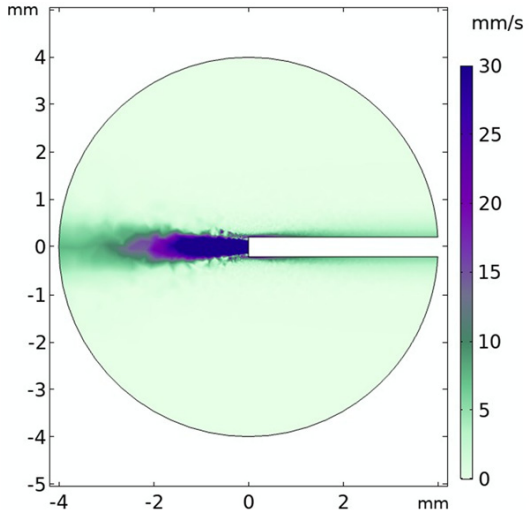

Figure 3. Single needle setup. Velocity map across the equatorial cross-section.

We start with modeling injection using only the central needle with the injection rate set at Q = 10 mm^3/s. The transport through the tumor shell follows the same transport model governed by the pressure gradient near the shell. Later, we will also consider the case of a reduced shell transport that could be augmented by addition of specially designed drainage needles.

Figures 2 and **3** show respectively the pressure and velocity maps across the equatorial cross-section for the single-needle injection. A pressure value of about 30 kPa at the needle tip is consistent with that measured in [18], and the velocity map exhibits a typical jet-like formation that was also seen in X-ray images published in [18]. As a result, the volume of the tumor tissue that is directly affected by the therapeutic is small, thus decreasing the efficiency of the medication.

An introduction of additional injection needles allows for a) increase of the volume of the tissue interacting with the medication and b) decrease of the injection-induced pressure. **Figures 4** and **5** show respectively the pressure and the flow velocity maps across the equatorial cross-section when the drug is delivered using all 7 needles (in this cross section only three needles are shown) with the same injec-

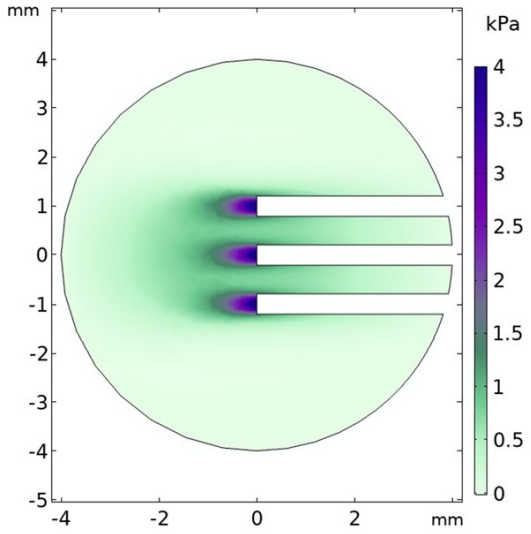

Figure 4. Multiple needle setup. Pressure map across the equatorial cross-section. In this cross-section, two (out of seven) additional needles are shown - one on the top and another on the bottom.

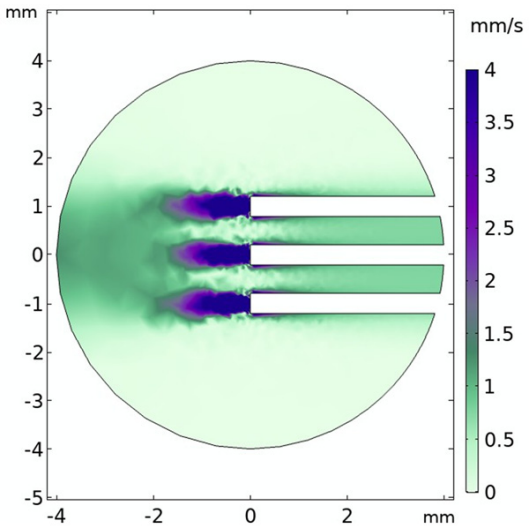

Figure 5. Multiple needle setup. Velocity map across the equatorial cross-section. In this cross-section, two (out of seven) additional needles are shown - one on the top and another on the bottom.

tion rate Q = 10 mm^3/s. As it could have been expected, a 7-fold drop in the maximum values of the pressure and velocity is observed.

Finally, we describe a setup that can be used to counter a reduced transport through the tumor boundary, in which case the pressure inside the tumor can increase substantially during injection. That can be remedied by introducing a drainage system consisting of several drainage needles with perforated or partially removed walls. In addition, by providing the outflow in the direction opposite to the injection, the flow geometry is affected in the way that further increases the volume occupied by the injectant. This setup is shown in **Figure 6** with the six drainage needles placed on a 2-mm radius circle around the central needle.

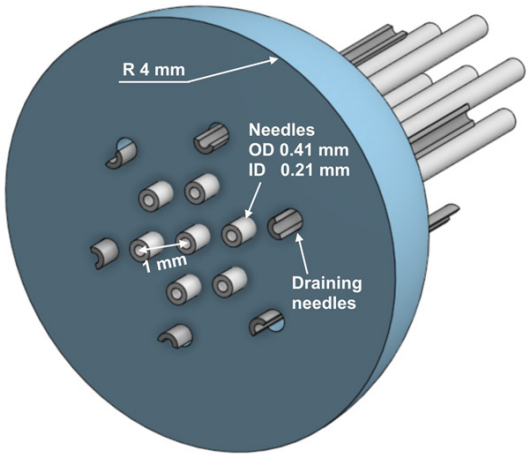

Figure 6. Multiple needle setup with drainage needles. The front part of the sphere is not shown for clarity. The tumor tissue is modeled by a porous media enclosed in a sphere with a radius of 4 mm. Thirteen 27-gauge needles with an OD of 0.41 mm and an ID of 0.21 mm are inserted with their tips positioned at the equatorial cross-section. The six needles surrounding the central needle are positioned on a circle with a radius of 1 mm. The six drainage needles are positioned on a circle with a radius of 2 mm. A half of the wall of each drainage needle is removed to provide for an unconstrained liquid outflow.

This arrangement is numerically simulated in the manner similar to that described in the previous section for a limit case of a completely opaque tumor wall. The flow velocity map shown in **Figure 7** illustrates the liquid flow that is now modified by being reflected from the wall and redirected to the drainage needles (top and bottom in this cross-section).

Conclusions

Our analysis clearly demonstrates that the model with a multi-needle injection (specifically, seven needles were considered) setup predicts a more homogeneous distribution of the injectant and decrease the pressure within a tumor compared to that for the single needle injection

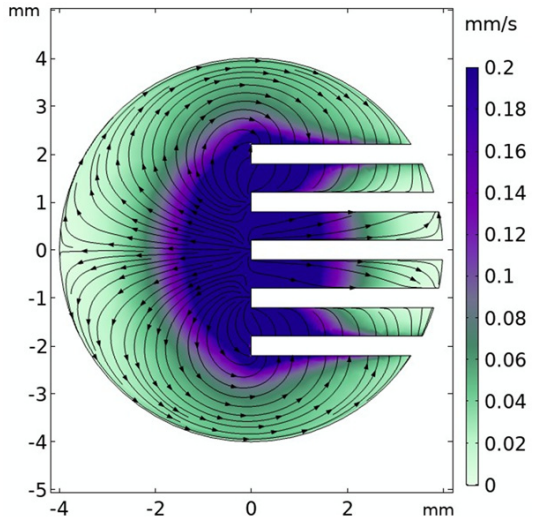

Figure 7. Multiple needle setup with a drain. Velocity map and flow streamlines. In this cross-section, two (out of six) drainage needles are shown - one on the top and another on the bottom.

case. Additional draining needles (six draining needles were considered) further improve the uniformity of the injectant and expand its volume. Although this analysis has utilized a very simplified transport model, such multi-needle injection approach could be used to optimize delivery of desired therapeutics to solid tumors and any parenchymal/solid tissues of mammalian body. Note here that simulation of needle insertion at random positions about the equatorial cross-section yielded very similar results. In addition, although a particular number of needles - 7 for the injection and 6 for the drainage - is used in this paper, our simulations indicated that a specific choice for the quantity of these needles is not important as a long as they cover a large fraction of the tumor cross-section.

Acknowledgements

This research did not receive any specific grant from funding agencies in the public, commercial, or not-for-profit sectors.

Disclosure of conflict of interest

None.

Address correspondence to: Vladimir Subbotin, 602 Samuel Drive, Madison, WI 53717, USA. E-mail: vladimir.m.subbotin@gmail.com

References

[1] Larkin J, Chiarion-Sileni V, Gonzalez R, Grob JJ, Cowey CL, Lao CD, Schadendorf D, Dummer R, Smylie M and Rutkowski P. Combined nivolumab and ipilimumab or monotherapy in untreated melanoma. N Engl J Med 2015; 373: 23-34.

[2] Weber J, Mandala M, Del Vecchio M, Gogas HJ, Arance AM, Cowey CL, Dalle S, Schenker M, Chiarion-Sileni V and Marquez-Rodas I. Adjuvant nivolumab versus ipilimumab in resected stage III or IV melanoma. N Engl J Med 2017; 377: 1824-1835.

[3] Barham W, Gicobi JK, Yan Y, Dronca RS and Dong H. Paradox-driven adventures in the development of cancer immunology and immunotherapy. Gen Dis 2019.

[4] Hargadon KM, Johnson CE and Williams CJ. Immune checkpoint blockade therapy for cancer: an overview of FDA-approved immune checkpoint inhibitors. Int Immunopharmacol 2018; 62: 29-39.

[5] Nevedomskaya E, Baumgart S and Haendler B. Recent advances in prostate cancer treatment and drug discovery. Int J Mol Sci 2018; 19: 29-39.

[6] Sun W. Recent advances in cancer immunotherapy. J Hematol Oncol 2017; 10: 96.

[7] Kroschinsky F, Stölzel F, von Bonin S, Beutel G, Kochanek M, Kiehl M and Schellongowski P. New drugs, new toxicities: severe side effects of modern targeted and immunotherapy of cancer and their management. Crit Care 2017; 21: 1-11.

[8] Puzanov I, Diab A, Abdallah K, Bingham C, Brogdon C, Dadu R, Hamad L, Kim S, Lacouture M and LeBoeuf N. Managing toxicities associated with immune checkpoint inhibitors: consensus recommendations from the Society for Immunotherapy of Cancer (SITC) Toxicity Management Working Group. J Immunother Cancer 2017; 5: 1-28.

[9] Yang L, Yu H, Dong S, Zhong Y and Hu S. Recognizing and managing on toxicities in cancer immunotherapy. Tumour Biol 2017; 39: 1-13.

[10] Zarifa A, Salih M, Lopez-Mattei J, Lee HJ, Iliescu C, Hassan S, Palaskas N, Durand JB, Mouhayar E and Kim J. Cardiotoxicity of FDA-approved immune checkpoint inhibitors: a rare but serious adverse event. JIPO 2018; 1: 68-77.

[11] Fransen MF, van der Sluis TC, Ossendorp F, Arens R and Melief CJ. Controlled local delivery of CTLA-4 blocking antibody induces CD8+ T-cell-dependent tumor eradication and decreases risk of toxic side effects. Clin Cancer Res 2013; 19: 5381-5389.

[12] Van De Voort TJ, Felder MA, Yang RK, Sondel PM and Rakhmilevich AL. Intratumoral delivery of low doses of anti-CD40 mAb combined with monophosphoryl lipid a induces local and systemic antitumor effects in immunocompetent and T cell-deficient mice. J Immunother 1997; 2013; 36: 29-40.
[13] Singh M, Vianden C, Cantwell MJ, Dai Z, Xiao Z, Sharma M, Khong H, Jaiswal AR, Faak F and Hailemichael Y. Intratumoral CD40 activation and checkpoint blockade induces T cell-mediated eradication of melanoma in the brain. Nat Commun 2017; 8: 1-10.
[14] Aznar MA, Tinari N, Rullan AJ, Sanchez-Paulete AR, Rodriguez-Ruiz ME and Melero I. Intratumoral delivery of immunotherapy-act locally, think globally. J Immunol 2017; 198: 31-39.
[15] Marabelle A, Kohrt H, Caux C and Levy R. Intratumoral immunization: a new paradigm for cancer therapy. Clin Cancer Res 2014; 20: 1747-1756.
[16] Marabelle A, Kohrt H and Levy R. Intratumoral anti-CTLA-4 therapy: enhancing efficacy while avoiding toxicity. Clin Cancer Res 2013; 19: 5261-5263.
[17] Carlson P. Consecutive injections in different tumor regions, without complete retraction the needle tip needle from tumor boundary. Personal Communication 2019.
[18] Comley K and Fleck N. Deep penetration and liquid injection into adipose tissue. J Mech Mater Struct 2011; 6: 127-140.
[19] Rasouli SS, Jolma IW and Friis HA. Impact of spatially varying hydraulic conductivities on tumor interstitial fluid pressure distribution. IMU 2019; 100175.
[20] Reddy NP and Cochran GV. Interstitial fluid flow as a factor in decubitus ulcer formation. J Biomech 1981; 14: 879-881.